Cyclic Boronates Inhibit All Classes of β-Lactamase

Samuel T. Cahill[a], Ricky Cain[d], David Y. Wang[a], Christopher T. Lohans[a], David W. Wareham[b], Henry P. Oswin[c], Jabril Mohammed[c], James Spencer[c], Colin W. G. Fishwick[d], Michael A. McDonough[a], Christopher J. Schofield[a†] & Jürgen Brem[a†]

[a]Chemistry Research Laboratory, University of Oxford, Oxford, UK

[b]Queen Mary University of London, London, UK

[c]School of Cellular and Molecular Medicine, University of Bristol, Bristol, UK

[d]School Of Chemistry, University of Leeds, Leeds, UK

[†]Corresponding author (Jürgen Brem email: jurgen.brem@chem.ox.ac.uk, Christopher Schofield email: christopher.schofield@chem.ox.ac.uk)

Abstract

β-Lactamase-mediated resistance is a growing threat to the continued use of β-lactam antibiotics. The use of the β-lactam-based serine-β-lactamase (SBL) inhibitors clavulanic acid, sulbactam, tazobactam, and, more recently, the non-β-lactam inhibitor avibactam has extended the utility of β-lactams against bacterial infections demonstrating resistance via these enzymes. These molecules are, however, ineffective against the metallo-β-lactamases (MBLs), which catalyse their hydrolysis. To date, there are no clinically available metallo-β-lactamase inhibitors. Co-production of MBLs and SBLs in resistant infections is, thus, of major clinical concern. The development of 'dual-action' inhibitors, targeting both SBLs and MBLs, is of interest, but these are considered difficult to achieve due to the structural and mechanistic differences between the two enzyme classes. We recently reported evidence

that cyclic boronates can inhibit both serine- and metallo-β-lactmases. Here we report that cyclic boronates are able to inhibit all four classes of β-lactamase, including the class A extended spectrum β-lactamase, CTX-M-15, the class C enzyme, AmpC from *Pseudomonas aeruginosa*, and class D OXA enzymes with carbapenem-hydrolysing capabilities. We demonstrate that cyclic boronates can potentiate the use of β-lactams against Gram-negative clinical isolates expressing a variety of β-lactamases. Comparison of a crystal structure of a CTX-M-15:cyclic boronate complex with structures of cyclic boronates complexed with other β-lactamases reveals remarkable conservation of the small molecule binding mode, supporting our proposal that these molecules work by mimicking the common tetrahedral anionic intermediate present in both serine- and metallo-β-lactamase catalysis.

Introduction

The β-lactam antibiotics remain the most important drug class for the treatment of bacterial infections (1). However, their continued use is jeopardized by the increasing spread of resistance mechanisms, including that mediated by β-lactamases, which, cumulatively, can hydrolyse all classes of β-lactam antibiotics (2). β-Lactamases can be divided into four classes (Ambler classes A, B, C and D (3)) and manifest considerable sequence and structural diversity as well as different, but overlapping, substrate profiles (4). The serine-β-lactamases (SBLs), classes A, C and D, likely evolved from the penicillin-binding protein (PBP) targets of β-lactam antibiotics (5-8). Among the SBLs the extended-spectrum SBLs (ESBLs) are of particular clinical concern. Their ability to hydrolyse extended spectrum cephalosporins and

the monobactam, aztreonam (9), is an important reason for failure of cephalosporin-based therapies (10). Of particular note are the CTX-M enzymes, which have become the most prevalent ESBLs worldwide (11). The SBL carbapenemases, such as variants of class D enzymes OXA-23 and OXA-48, are a growing concern, since they are able to hydrolyse carbapenems, which have often been used as the last line of antibacterial defence (12). Inhibitors of the SBLs include the β-lactams clavulanic acid, sulbactam and tazobactam, which are active against class A β-lactamases (2, 13, 14), and the recently introduced non-β-lactam β-lactamase inhibitor, avibactam, which has a broader spectrum of SBL inhibition activity (15, 16). These inhibitors have increased the efficacy of β-lactam antibiotics against SBL-mediated resistance in bacteria, but they are inactive against the Zn(II)-dependent class B metallo-β-lactamases (MBLs), which constitute a structural and mechanistically distinct family of enzymes and exhibit considerable heterogeneity, even amongst themselves (17). The MBLs are able to hydrolyse all classes of β-lactam except for monobactams (18). The ability of the MBLs to hydrolyse SBL inhibitors, including avibactam (19), is a growing problem in the treatment of infections where both SBL- and MBL-mediated cephalosporin and carbapenem resistance have been acquired (20). To date there are no clinically approved MBL inhibitors.

As a consequence of increasing variation in the β-lactamase-mediated resistance to β-lactam antibiotics, the development of broad-spectrum inhibitors of both the SBLs and MBLs is of considerable interest. This is presently perceived to be challenging due to the mechanistic and structural differences between the SBLs and MBLs. We have recently reported that cyclic boronates can inhibit representatives of class A, B, and D β-lactamases (21). Cyclic boronates act as analogues of the first tetrahedral intermediate that is common to both SBLs and MBLs. Here we show that cyclic boronates are able to inhibit all classes of

β-lactamase, including the class A ESBL, CTX-M-15, the class C enzyme, AmpC from *Pseudomonas* aeruginosa, and two carbapenem-hydrolysing OXA variants, OXA-23 and OXA-48. These cyclic boronates are effective in inhibiting the growth of clinical Gram-negative bacterial strains expressing multiple β-lactamases. Crystallographic analysis of a cyclic boronate complexed with CTX-M-15 supports the proposal that the cyclic boronates closely mimic the first tetrahedral intermediate in bicyclic β-lactam hydrolysis.

Materials and Methods

Cloning

Serine β-lactamases were amplified by direct PCR from producer bacterial strains and expressed as N-terminal hexahistidine fusions from the T7 vector pOPINF (22). CTX-M-15 was amplified from *E. coli* strain EO516 (kind gift of Prof. Neil Woodford, Public Health England) (23); *P. aeruginosa* AmpC was amplified from strain PAO1 (kind gift of the former Pseudomonas genetic stock center, East Carolina University) (24); OXA-23 and OXA-48 were amplified from clinical *Acinetobacter baumannii* and *Klebsiella pneumoniae* isolates (kind gifts of Prof. Timothy Walsh and Dr. Mark Toleman, Cardiff University). β-lactamase open reading frames encoding the mature polypeptides (i.e with regions encoding the signal peptide removed) were amplified by PCR using Phusion polymerase (New England Biolabs) and primers as detailed in Supplementary Table S1. PCR products were cloned into the pOPINF T7 expression vector (22), linearized at the KpnI and HindIII sites, using the InFusion recombinase system (Clontech) (25), transformed into *E. coli* Stellar (Clontech) and positive clones selected by blue-white screening. Recombinant plasmids were purified and

sequenced (Eurofins Genomics) to confirm identity with published sequences and that no mutations had been introduced during the cloning procedure. The resulting expression constructs encode (exclusive of vector derived amino acid residues) mature β-lactamase sequences starting at residues 29 (CTX-M-15), 27 (AmpC), 18 (OXA-23) and 22 (OXA-48).

Enzyme production

Recombinant CTX-M-15, AmpC, OXA-23 and OXA-48, each with an *N*-terminal His-tag, were produced in *E. coli* BL21(DE3) cells using auto-induction medium supplemented with 50 µg mL^{-1} ampicillin. Cells were grown for four hours at 37 °C before cooling to 18 °C and continuing growth overnight. Cells were harvested by centrifugation (10 min, 10000 *g*), resuspended in 50 mL lysis buffer (50 mM HEPES, pH 7.5, 500 mM NaCl, 5 mM imidazole), supplemented with DNAse I, and lysed by sonication. The supernatant was loaded onto a 5 mL HisTrap HP column followed by extensive washing with 50 mM HEPES, pH 7.5, 500 mM NaCl, 5 mM imidazole before elution with a 20–500 mM imidazole gradient. Fractions containing purified enzyme were concentrated by centrifugal ultrafiltration (Amicon Ultra - 15 mL, 10 kDa MWCO, Millipore). The resultant solution was injected onto a Superdex S200 column (300 mL) and eluted with 50 mM HEPES, pH 7.5, 200 mM NaCl. Fractions containing pure His-tagged enzyme were incubated overnight at 4 °C with His-tagged 3C protease (1:100 w/w) to remove the *N*-terminal His-tag. The 3C protease together with any uncleaved protein the digestion mixture was removed by use of a second HisTrap HP column pre-equilibrated with 50 mM HEPES, pH 7.5, 500 mM NaCl, 20 mM imidazole. Purified enzyme fractions as identified by SDS-PAGE, were pooled and concentrated by centrifugal ultrafiltration before buffer exchange into 25 mM HEPES, pH 7.5, 100 mM NaCl. The concentrations of the purified proteins were determined using a NanoDrop ND-1000

spectrophotometer (Thermo Scientific, ε = 25440, 61310, 43430 or 63940 M^{-1} cm^{-1} for CTX-M-15, AmpC, OXA-23 and OXA-48, respectively).

Recombinant TEM-1 (26) with an *N*-terminal His-tag, VIM-1 (27) with a 3C-cleaved *C*-terminal His-tag, and OXA-10 (28) were produced as previously described. The concentrations of the purified proteins were determined using a NanoDrop ND-1000 spectrophotometer. Thermo Scientific, (ε = 27960, 29910, or 48930 M^{-1} cm^{-1} for TEM-1, VIM-1, and OXA-10, respectively)

^{13}C-Labelling of OXA-10 Enzyme

The ^{13}C labelling of carbamylated lysine was based on a literature protocol (29). Purified OXA-10 enzyme was first dialyzed overnight against degassed 25 mM sodium acetate, pH 4.5, 0.1 mM EDTA, then overnight against 50 mM sodium phosphate, pH 7.4, 0.1 mM EDTA, 1 mM $NaH^{13}CO_3$ (Sigma-Aldrich). The enzyme was then dialyzed overnight against 50 mM sodium phosphate, pH 7.4, 0.1 mM EDTA, 10 mM $NaH^{13}CO_3$, aliquoted, and frozen using liquid N_2.

Inhibition assays

Inhibition assays were carried out using FC5 as a fluorogenic reporter substrate (30). Enzyme concentrations and buffers were the same as those employed in steady-state kinetic studies (Table S2). TEM-1, BcII and VIM-1 were screened at 1 nM, 500 pM and 125 pM, respectively. The concentration of FC5 employed was 10 µM for TEM-1 and 5 µM for all other enzymes. IC_{50} values were determined by pre-incubating the enzyme with the inhibitor in the assay buffer at room temperature for 10, 30, 60 or 300 minutes prior to the addition of substrate. Data at 0 minutes incubation were obtained by addition of enzyme

into a pre-mixed solution of inhibitor and substrate. Residual enzyme activity was determined for a range of inhibitor concentrations. Non-linear regression fitting of IC_{50} curves was carried out using a three-parameter dose-response curve in GraphPad Prism. Errors in IC_{50} are expressed as: $\frac{\sigma(\log IC_{50})}{\log IC_{50}} \times IC_{50}$.

Antimicrobial Susceptibility Testing

The *in vitro* activity of **2** was assessed using nine clinical isolates carrying multiple β-lactamases (Table 3). Isolates selected included *Enterobacteriaceae* (*E. coli* ST 131*, Klebsiella pneumoniae* ST 258*, Providencia stuartii*) producing class A ESBLs (CTX-M-15, CTX-M-27, SHV-5, VEB-1), serine (KPC-2) and metallo-carbapenemases (VIM-1, VIM-2), plasmid mediated AmpC (CMY-2) and/or carbapenem-hydrolysing OXA-48-like oxacillinases (OXA-181, OXA-232) in various combinations. The activity against carbapenemase producing strains of *Pseudomonas aeruginosa* (VIM-2) and *Acinetobacter baumannii* (OXA-23) was also investigated. All isolates have previously undergone extensive phenotypic and genotypic characterisation (31).

Bacterial susceptibility to β-lactams and standard β-lactam inhibitor (clavulanic acid (CLAV), sulbactam (SUL), and tazobactam (TAZ)) combinations was determined by broth microtitre dilution (BMD) according to the Clinical Laboratory Standards Institute (CLSI) methodology (32). MICs were determined using commercial Sensititre GN4F panels (Thermo Scientific, UK, LOT B55051) and Mueller-Hinton II cation adjusted broth (Oxoid, UK), with and without the addition of **2** at a fixed concentration of 10 µg/ml. Plates were incubated at 37 °C for 18 hrs and MICs read by eye following the addition of Alamar Blue reagent *(Trek Diagnostics)*.

The inhibitory effects of **2** on susceptibility to 19 diverse β-lactam compounds was also assessed in Kirby-Bauer disc diffusion tests. Combination discs (Oxoid) were prepared with a fixed ratio of 2:1 between the β-lactam (μg) and **2**. Zones of inhibition were compared around combined and un-supplemented discs following overnight incubation on MH II plates.

NMR Spectroscopy

^{13}C NMR experiments used a Bruker AVIII 600 MHz spectrometer equipped with a Prodigy broadband cryoprobe. Spectra were acquired at 298 K using a standard Bruker ^{13}C pulse sequence. The experimental parameters used were: 2048 scans, 36058 Hz spectral width, 2.0 s relaxation delay, and 65536 data points. A line broadening of 10 Hz was applied to all spectra. NMR samples contained 560 μM OXA-10 and 10 mM $NaH^{13}CO_3$, and were supplemented with 10% D_2O. The impact of boronate **1** was tested at a concentration of 5 mM.

Crystallisation, X-ray data collection and processing

Crystallisation experiments were set up using a 13 mg mL^{-1} solution of CTX-M-15 in 50 mM HEPES, pH 7.5, 100 mM NaCl supplemented with 10 mM **1**. Crystallisation was performed at room temperature using sitting drop vapour diffusion methods. Crystals were obtained after two days using 100 μL of 100 mM HEPES, pH 7.5, 70% 2,4-methylpentanediol in the reservoir and a 1:2 mixture (1 μL:2 μL) of protein to reservoir solution in the crystallisation drop. Crystals were cryo-protected using 25% glycerol in reservoir solution before harvesting with nylon loops and flash-cooling in liquid nitrogen. Diffraction data were collected at 100 K using a Rigaku FRE+ Superbright diffractometer. Diffraction data were

integrated and scaled using HKL3000 (33). The structure was solved by molecular replacement with Phaser (34) using a published structure (PDB accession code: 4HBT(35)) as a search model. The structure was then fit and refined iteratively using PHENIX and Coot (36, 37).

Structural energy minimisation

Energy minimisation of small molecule structures was performed using the MM2 energy minimisation function in ChemBio3D Ultra (38).

Results

Cyclic boronate inhibition of serine-β-lactamases and metallo-β-lactamases

To investigate the extent to which cyclic boronates inhibit class C β-lactamases as well as the important class A ESBL and class D carbapenemase targets, we used a fluorogenic assay (30) to screen the cyclic boronates, which we have found to inhibit other β-lactamases (21), against them. The β-lactamases used for screening included TEM-1, CTX-M-15 (class A), the MBL from *Bacillus cereus*, BcII, Verona integron-encoded metallo-β-lactamase 1, VIM-1 (class B), AmpC from *Pseudomonas aeruginosa* (class C), OXA-23 and OXA-48 (class D), collectively representing all classes of β-lactamase. (For comparison with other relevant publications, we also screened CTX-M-15, AmpC, OXA-23, and OXA-48 with the commonly used reporter substrate nitrocefin (39), Table S2). To benchmark the potency of the cyclic boronates we also screened the clinically used SBL inhibitors avibactam (MedChemexpress LLC) (16, 40), sulbactam (41, 42), and BLI-489, a potent inhibitor of class D enzymes (2, 43,

212 44). For MBLs we used the broad-spectrum thiol-based MBL inhibitors L-captopril (45, 46)
213 and (racemic) thiomandelic acid (47, 48) (Tables 1 & 2, see Figure S1 for structures of the
214 inhibitors). Since variations in the rate of reaction with, at least, avibactam has been
215 reported among the SBLs (16), we also investigated the time courses of inhibition by these
216 compounds over six hours.

217 Both cyclic boronates **1** and **2** exhibit inhibition against all five of the SBLs tested with
218 IC_{50} values ranging from 250 to 2 nM (Table 1). **1** and **2** exhibit a similar inhibition potency
219 against TEM-1 and CTX-M-15, **2** shows around 10-fold lower IC_{50} values than **1** against AmpC
220 (9.8 ± 0.3 nM vs 120 ± 10 nM, respectively, with 10 minutes pre-incubation) while **1** exhibits
221 10- to 15-fold lower IC_{50}s than **2** against the OXA enzymes (250 ± 1 nM vs 2600 ± 100 nM
222 after 10 minutes incubation for OXA-23 and 160 ± 1 nM vs 2600 ± 200 nM after 10 minutes
223 incubation for OXA-48). Against TEM-1 and CTX-M-15, **1** and **2** show similar potency to
224 avibactam and BLI-489, with IC_{50} values of low nanomolar to sub-nanomolar levels. Against
225 AmpC, **2** shows a similar potency to avibactam while **1** exhibits up to 60-fold lower IC_{50}
226 values than avibactam (9.8 ± 0.3 nM and 190 ± 10 nM at 10 minutes, respectively) with
227 results comparable to those for BLI-489 (30 ± 1 nM at 10 minutes). Neither **1** nor **2** were
228 able to achieve potency comparable with the lowest IC_{50} values exhibited by avibactam and
229 BLI-489 against the OXA enzymes, with IC_{50} values for **1** being around 10 to 20-fold higher
230 and those for **2** being around 100 to 200-fold higher .

231 The time-dependency of inhibition was found to vary depending on the particular
232 inhibitor-enzyme combination examined (Table 1). Where substantial time dependency in
233 the inhibition was observed, the largest decrease in IC_{50} generally manifested over the first
234 10 minutes of inhibition. Avibactam showed time-dependency in its inhibition of all the
235 tested SBLs with the lowest IC_{50} value typically achieved after 60 or 360 minutes pre-

incubation. The IC_{50} values obtained with BLI-489 only showed substantial time-dependency with CTX-M-15 and AmpC, with the lowest IC_{50} values seen after longer incubation times, as seen with avibactam. The time-dependency of inhibition by the cyclic boronates was similar to that observed for BLI-489 (i.e. seen with CTX-M-15 and AmpC but not with TEM-1 or the OXA enzymes) (Table 1). For CTX-M-15, a significant increase in the IC_{50} values for avibactam and BLI-489 was observed between 60 and 360 minutes of incubation. This may be the result of slow hydrolysis of the inhibited acyl-enzyme to restore a small population of active enzyme.

We also screened the cyclic boronates against the model MBL, BcII, and VIM-1 using the FC5-based fluorogenic assay (30). In all cases the inhibition of the MBLs by **2** was around 10 times more potent than by **1** (Table 2). **1** exhibited IC_{50} values around two- to five-fold lower than those seen with L-captopril. **2** showed very similar potency to thiomandelic acid against BcII but showed five to 10-fold greater potency than thiomandelic acid against VIM-1. No time-dependency of MBL inhibition by either the cyclic boronates or thiol-based inhibitors was observed (Table 2).

Susceptibility of clinical isolates to cyclic boronate 2

Consistent with our previous work (21), **2** was observed to be the more potent inhibitor of the isolated MBLs, compared to **1**. Since potency against different types of MBL is a highly desirable characteristic in the design of MBL/SBL dual inhibitors, **2** (10 μg/mL) was thus tested in combination with a number of β-lactams against a variety of Gram-negative clinical isolates known to produce multiple β-lactamases. Susceptibility to the monobactams aztreonam (AZT) and cephalosporins (ceftriaxone (CRO), ceftazidime (CAZ), and cefepime (FEP)) was either increased or completely restored to strains producing CTX-M-1-like (CTX-

M-15, CTX-M-27) enzymes. MICs to ampicillin (AMP) and piperacillin (PIP) in combination with fixed ratios of clavulanic acid (CLAV), sulbactam (SUL), and tazobactam (TAZ) were also lower for CTX-M containing isolates but not significantly in those also producing an OXA (OXA-1, OXA-181, OXA-23) or plasmid-borne AmpC (CMY-4) enzyme. For *Enterobacteriaceae* producing MBLs, heightened activity was seen with carbapenems against VIM-4 producing *K. pneumoniae* and VIM-1 producing *P. stuartii.* There were less marked effects on cephalosporin MICs, presumably due to co-production of SHV and VEB-like ESBLs and hyper-expression of chromosomal AmpC in these isolates. In strains with OXA-like carbapenem-hydrolysing class D β-lactamases (CHDLs), carbapenem susceptibility was increased in *E. coli* producing the OXA-181 variant, in combination with CTX-M-15 and CMY-4, but not against a multi-drug resistant *K. pneumoniae* producing the OXA-232 variant in association with CTX-M-15 and multiple other class SHV ESBLs. Of note, no significant effects of **2** were seen on the carbapenem susceptibility of either VIM-2 producing *P. aeruginosa* or *A. baumannii* with OXA-23 (Table 3)

Disc diffusion screens in which **2** was added in a fixed ratio against the same strains revealed some interesting findings on its potential as an inhibitor (Supplemental Disc Diffusion Test Images). In *Enterobacteriacae*, **2** generally enhanced the activity of PIP, AZT, cefoxitin (FOX), cefotaxime (CTX) and CAZ in those without OXA-CHDLs. The effects on carbapenems were clearly observed for the VIM-4 producing strains at the 2:1 ratio.

^{13}C NMR study with OXA-10

For the class D OXA enzymes, the active site lysine (Lys70) is carbamylated via non-enzymatic reaction with carbon dioxide (49). This residue is critical for the activity of the enzymes and acts as a general acid/base during β-lactam hydrolysis (29). Since the

carbamylation of Lys70 is reversible, it is possible to site-specifically label the residue with ^{13}C, via incubation with a ^{13}C bicarbonate buffer. This labelling allows for changes of the active site, for example inhibitor binding, to be studied using NMR (29). Using this reported technique, we labelled the carbamylated Lys70 of OXA-10 with ^{13}C (using $NaH^{13}CO_3$) in order to monitor binding of the cyclic boronate **1** within the active site of the enzyme (Figure S6). Upon binding of the inhibitor, a 6 ppm shift in the ^{13}C-labelled carbamylate signal is observed.

Crystal structure of 2 bound to CTX-M-15

Crystal structures of the cyclic boronates **1** and **2** in complex with class B and D β-lactamases (BcII and VIM-2, and OXA-10, respectively) and PBP-5 from *E. coli* have been reported (21); however, structural information on inhibition of the clinically important class A β-lactamases, in particular ESBLs, by cyclic boronates has not been described. We thus worked to obtain a structure of the ESBL CTX-M-15:**1** complex, which diffracted to 1.95 Å resolution (See Table S4 for crystallographic data). The structure was solved by molecular replacement using the reported structure of the apo-enzyme (PDB accession code: 4HBT (35)) as a search model. The overall structure of the CTX-M-15:**1** complex is highly similar to that of the search model with an RMSD of 0.194 Å over Cα atoms. In a similar fashion to that seen in a CTX-M-15:Avibactam complex crystal structure (PDB accession code: 4S2I (50)), comparison with the apo-enzyme reveals no remarkable changes in the positions of the backbone or amino acid side chains upon reaction with cyclic boronate **1**.

Analysis of the electron density maps clearly reveals **1** as bound at the active site via reaction with the side chain of Ser73 (Figure 2A). In an analogous manner to the structures of OXA-10 and PBP-5 with **2** (21), PDB accession codes 5FQ9 and 5J8X, respectively, the

electron density map provides clear evidence for tetrahedral coordination of the boron atom (Figure S7). Aside from the covalent reaction with Ser73, **1** is positioned to form hydrogen bonding interactions with the side chains of Lys76, Asn107, Ser133, Asn135, Thr238 and Ser240 as well as backbone atoms of Ser73, and Ser240 and three nearby water molecules, Waters 4, and 116. In addition there is a hydrophobic/aromatic interaction between the sidechain of Tyr108 and the planar aromatic ring of the ligand. Interestingly, and as seen in the CTX-M-15:avibactam complex (50), a water molecule is observed in the CTX-M-15:**1** complex which occupies the same position as the water responsible for hydrolysis of the acyl-enzyme intermediate in CTX-M-15-catalysed β-lactam hydrolysis, Wat4 in Figures 2 and S6 (35).

We then compared the conformation of the cyclic boronate **1** in CTX-M-15 with those observed in MBLs (BcII, PDB accession code: 5FQB, and VIM-2, PDB accession code: 5FQC), and OXA-10 (PDB accession code: 5FQ9) as well as PBP-5 (PDB accession code: 5J8X). Although there are some variations in the precise orientations of the C-7 cyclohexyl amide/aromatic acetamide side chain, the conformation of the fused bicyclic boronate ring system is remarkably well conserved across all the structures analysed (Figure 2C). In support of the proposal that the cyclic boronates mimic the first tetrahedral intermediate in β-lactam hydrolysis, which is common in both SBL and MBL catalysis, small molecule energy minimisation studies on **2** and the tetrahedral species produced by addition of a hydroxide ion onto the β-lactam carbonyl of cefalexin, reveal strong structural similarity between the two species.

Discussion

The results reveal that cyclic boronates **1** and **2**, which are based on β-lactamase inhibitors described in patent literature (51), are able to inhibit all classes of β-lactamase, including the important clinically relevant ESBL CTX-M-15 and the OXA carbapenemases, as well as AmpC from *P. aeruginosa*, with low micromolar to low nanomolar IC_{50} ranges (Tables 1 & 2). The compounds show similar inhibition potency to avibactam against TEM-1, CTX-M-15 and AmpC. **1** was the more potent of the two cyclic boronates against the OXA enzymes, but was unable to achieve the potency of avibactam against these enzymes (16). However, the fact that the described cyclic boronate scaffold has yet to be optimised suggests that greater potency should be possible for cyclic boronates against the class D β-lactamases, in line with that seen for other classes. Interestingly, NMR data acquired with OXA-10 show that carbamylation of the active site lysine is maintained upon binding of boronate **1** (Figure S6). The observed shift of 6 ppm is substantial when compared to that observed upon binding of hydroxyisopropylpenicillanates, where a shift of 0 to 0.4 ppm is observed (52). The greater shift of the ^{13}C signal on binding of the boronate likely reflects the different environment of the active site serine – being bound to an sp^3 anionic boron centre when complexed to **1** as opposed to an sp^2 carbon centre in the hydroxyisopropylpenicillanate complex.

Time courses of inhibition against the SBLs reveal that time-dependence in IC_{50} value is manifest, the magnitude of which is dependent on the enzyme-inhibitor combination employed. This observation is consistent with potential variations in acylation rates seen with avibactam (16) and the SBLs as well as 'on-enzyme' fragmentation/cross-linking reactions that can occur subsequent to acylation, as demonstrated, for example, in the case

of sulbactam (41, 42) and BLI-489 (53). Notably TEM-1 and CTX-M-15 appear to manifest differences in the time-dependency of their inhibition by all five of the tested inhibitors, as has been previously demonstrated for the response of TEM-1 and CTX-M-9 to clavulanic acid, sulbactam and tazobactam (54), emphasising the variation in the properties of the β-lactamases even within the same class (5).

1 and **2** exhibit sub-micromolar IC_{50}s against the MBLs, BcII and VIM-1 with **2** being the more potent compound against both enzymes. Inhibition of BcII by **2** is comparable in potency to thiomandelic acid, while **2** is around 10 times more potent than thiomandelic acid against VIM-1. Avibactam is a potent inhibitor of SBLs but, notably, is hydrolysed slowly by some MBLs (19, 55). Time courses of cyclic boronate inhibition against the enzymes tested demonstrated no time-dependence for inhibition of the MBLs, at least under our experimental conditions. Despite avibactam being a potent inhibitor of SBLs, it is able to be hydrolysed by MBLs (19), suggesting potential problems in the long-term clinical use of avibactam (and other inhibitors working by acylation) as resistance mediated by combinations of SBLs and MBLs become more prevalent (20). In contrast, no β-lactamase-catalysed turnover of the cyclic boronates has been seen (as expected) and, to date, we have no evidence for these compounds binding to β-lactamases or PBPs in a ring-opened fashion. This is consistent with a recent publication suggesting that, at least for 6-membered boronate rings, the closed form is the dominant species in solution (56).

Cyclic boronate **2** potentiated the activity of all four classes of β-lactam against Gram-negative clinical isolates (Table 3). Co-administration of **2** alongside clinically used SBL inhibitors clavulanic acid, sulbactam and tazobactam was able to further potentiate the activity of penicillins against some *E. coli* strains (EC107 and EC113) when compared to co-administration with the SBL inhibitors alone. **2** also increased the effectiveness of both

379 cephalosporins and carbapenems against VIM-producing *K. pneumoniae* strains, although
380 this result is not apparent with KP41 – possibly due to the sheer number of β-lactamases
381 (six) being produced. Activity against the VIM-2-producing *P. aeruginosa* was also limited.
382 Mechanisms of multi-drug resistance in this strain have not yet been fully elucidated,
383 although production of the native AmpC β-lactamase combined with upregulated efflux and
384 permeability lesions are likely to be involved. An increased susceptibility to ceftolozane was
385 a common finding regardless of the number or class of β-lactamase produced, except in *A.*
386 *baumannii*. Ceftolozane is a 5th generation cephalosporin, recently developed for use in
387 combination with tazobactam (57). The limited isolate results presented here suggest that
388 ceftolozane, partnered with a cyclic boronate, could be an attractive β-lactam/inhibitor
389 combination to pursue in future.

390 A structure of the CTX-M-15:**1** complex reveals a conserved mode of binding for this
391 inhibitor, very similar to our previously reported structures, with a tetrahedral boron centre
392 and the closed bicyclic scaffold maintained as in our previously reported work (21).
393 Comparison of our structure with that of CTX-M-15 in complex with RPX-7009, a boron-
394 based SBL inhibitor currently in phase III clinical trials (58, 59), and a TEM-1:BJH (60)
395 complex reveals a striking similarity in the mode of binding for these related scaffolds
396 (Figure S8). Interestingly, the latter structure was interpreted as an acyclic boronate binding
397 mode, despite the compound being able to adopt a near identical bicyclic conformation to
398 our inhibitors via reaction of its phenolic oxygen with the boron centre (Figure S8C) (60). It
399 should be noted that, in contrast to the structural conservation observed for the cyclic
400 boronate complex conformations, there is considerably more variation in the structural
401 conformations of acyl-enzyme (and product) complexes formed by the reaction of SBLs with
402 β-lactams, and of reported product/intermediate complexes formed from MBLs and β-

lactams (Figure S9) (29, 61-63). Since more conformational flexibility might be anticipated once the β-lactam ring has been opened, this analysis supports the proposal that the cyclic boronates best mimic the first tetrahedral intermediate (i.e. acts as "transition-state" analogues).

The cyclic boronate scaffold is thus able to potently inhibit all classes of β-lactamase by adopting an enzyme:inhibitor complex that mimics a tetrahedral intermediate in β-lactam hydrolysis. With further optimisation cyclic boronates could form a new family of clinically useful β-lactamase, and maybe other hydrolytic enzyme, inhibitors. In addition to their inhibitory properties the cyclic boronates also provide important structural and mechanistic insights into the nature of β-lactamase:β-lactam complexes allowing us to build a more detailed picture of more transient species that have yet to be structurally characterised.

With the first cyclic boronate drug, tavaborole (64), approved for clinical use in the treatment of external fungal infections and further cyclic boronates in the pipeline as anti-inflammatory and anti-bacterial treatments (65, 66), the use of cyclic boronates as future drug candidates seems to be an inevitability. The ability of these molecules to mimic tetrahedral intermediates in enzyme-catalysed hydrolysis pathways may prove to be highly useful in the inhibition of mechanistically diverse enzymes, as exhibited by the ability of **1** and **2** to inhibit all classes of β-lactamase, including serine-, metallo-, or other enzymes. In addition, similar classes of compounds such as cyclic phosphonates, sulfonates, and sulfonamides have yet to be extensively explored and may prove a fruitful source of future inhibitors.

Antimicrobial Agents and Chemotherapy

Accession Number

Coordinates and structure factors have been deposited in the Protein Data Bank with accession number 5FQA.

Declarations of interest

The authors declare no conflict of interest.

Funding Information

We thank the Biotechnology and Biological Sciences Research Council (grant number BB/J014427/1) and the Medical Research Council/Canadian grant (G1100135) for funding our work. We are grateful for assistance from the MRC SWON Alliance.

Tables & Figures

Inhibitor	Pre-incubation Time (min)	TEM-1 IC_{50} (nM)	CTX-M-15 IC_{50} (nM)	AmpC IC_{50} (nM)	OXA-23 IC_{50} (nM)	OXA-48 IC_{50} (nM)
1	0	2.6 ± 0.1	92 ± 6	68 ± 3	220 ± 1	140 ± 1
	10	1.3 ± 0.1	13 ± 1	9.8 ± 0.3	250 ± 1	160 ± 1
	30	1.6 ± 0.1	3.7 ± 0.1	4.5 ± 0.1	260 ± 1	170 ± 1
	60	1.5 ± 0.1	1.7 ± 0.1	2.6 ± 0.1	270 ± 1	170 ± 1
	360	1.7 ± 0.1	4.0 ± 0.01	2.4 ± 0.1	730 ± 2	270 ± 1
2	0	8.1 ± 0.1	39 ± 2	270 ± 60	2000 ± 100	2000 ± 100
	10	3.4 ± 0.1	7.5 ± 0.3	120 ± 10	2600 ± 100	2600 ± 200
	30	2.6 ± 0.1	2.8 ± 0.1	150 ± 10	3300 ± 200	3400 ± 100
	60	2.6 ± 0.1	1.3 ± 0.1	100 ± 10	2600 ± 100	3000 ± 100
	360	2.1 ± 0.1	6.4 ± 0.1	96 ± 1	3300 ± 200	3300 ± 200
Sulbactam	0	860 ± 80	44 ± 1	$> 2 \times 10^5$	$> 2 \times 10^5$	$> 2 \times 10^5$
	10	600 ± 200	29 ± 1	42000 ± 2000	$> 2 \times 10^5$	$> 2 \times 10^5$
	30	600 ± 200	28 ± 7	8600 ± 600	$> 2 \times 10^5$	$> 2 \times 10^5$
	60	500 ± 200	32.0 ± 0.3	4400 ± 500	$> 2 \times 10^5$	$> 2 \times 10^5$
	360	700 ± 300	16.6 ± 0.1	1000 ± 400	$> 2 \times 10^5$	$> 2 \times 10^5$
Avibactam	0	19 ± 1	9.9 ± 0.2	1400 ± 400	770 ± 4	2500 ± 30
	10	3.4 ± 0.1	1.1 ± 0.1	190 ± 10	390 ± 1	810 ± 50
	30	2.2 ± 0.1	0.40 ± 0.06	200 ± 10	160 ± 2	300 ± 2
	60	2.0 ± 0.1	0.39 ± 0.01	200 ± 10	71 ± 1	150 ± 1
	360	4.3 ± 0.1	6.4 ± 0.1	150 ± 10	13 ± 1	20 ± 1
BLI-489	0	4.8 ± 0.2	32 ± 2	210 ± 20	5.6 ± 0.1	14 ± 1
	10	2.0 ± 0.1	6.9 ± 0.2	30 ± 1	5.6 ± 0.1	15 ± 1
	30	1.7 ± 0.2	2.2 ± 0.1	12.0 ± 0.4	6.2 ± 0.1	16 ± 1
	60	1.7 ± 0.1	0.94 ± 0.03	5.6 ± 0.1	8.6 ± 0.1	22 ± 1
	360	1.9 ± 0.1	8.0 ± 0.1	1.9 ± 0.1	18 ± 1	49 ± 1

Table 1. Time course for the inhibition of serine-β-lactamases (classes A, C and D) by boronates 1 and 2 and established inhibitors that act by formation of a stable acyl-enzyme complex, using FC5 as a substrate (30). IC_{50} values were taken after pre-incubation of the enzyme with the corresponding inhibitor for 0, 10, 30, 60 or 360 minutes prior to assay. IC_{50} values were obtained from fitting of residual activity plots using GraphPad Prism.

Inhibitor	Pre-incubation Time (min)	BcII pH 7.5 IC_{50} (μM)	BcII pH 6.5 IC_{50} (μM)	VIM-1 pH 7.5 IC_{50} (μM)
1	0	2.8 ± 0.2	3.3 ± 0.1	1 ± 1
	10	3.0 ± 0.2	3.8 ± 0.2	1 ± 1.2
	30	2.8 ± 0.3	3.5 ± 0.1	1 ± 1.5
	60	3.4 ± 0.3	3.8 ± 0.2	1.4 ± 0.3
	360	3.1 ± 0.2	3.0 ± 0.2	1.2 ± 0.3
2	0	0.45 ± 0.02	0.27 ± 0.02	0.061 ± 0.001
	10	0.45 ± 0.02	0.20 ± 0.01	0.085 ± 0.002
	30	0.36 ± 0.02	0.20 ± 0.01	0.088 ± 0.001
	60	0.36 ± 0.01	0.20 ± 0.01	0.083 ± 0.002
	360	0.36 ± 0.03	0.23 ± 0.01	0.061 ± 0.001
L-Captopril	0	13.7 ± 0.3	17.4 ± 0.3	1.91 ± 0.06
	10	21 ± 1	20.4 ± 0.6	2.3 ± 0.2
	30	12.5 ± 0.5	16.8 ± 0.8	2.4 ± 0.2
	60	14.6 ± 0.4	13.7 ± 0.7	2.6 ± 0.1
	360	15 ± 1	16.3 ± 0.5	2.8 ± 0.2
(±)-Thiomandelic Acid	0	0.30 ± 0.03	0.27 ± 0.06	0.38 ± 0.03
	10	0.39 ± 0.05	0.9 ± 0.1	0.45 ± 0.02
	30	0.33 ± 0.04	0.5 ± 0.1	0.8 ± 0.9
	60	0.5 ± 0.2	2 ± 1	1.4 ± 0.9
	360	2 ± 1	2 ± 1	2 ± 1

Table 2. Time course for the inhibition of metallo-β-lactamases by boronates 1 and 2 and broad-spectrum thiol-based MBL inhibitors, using FC5 as a substrate (30). IC_{50} values were taken after pre-incubation of the enzyme with the corresponding inhibitor for 0, 10, 30, 60 or 360 minutes prior to assay. IC_{50} values were obtained from fitting of residual activity plots using GraphPad Prism.

Antimicrobial Agents and Chemotherapy

Bacterial Isolate	β-Lactmases Produced (Ambler Class)	± 2 Supplement (10 mg/L)	MIC (mg/L) for β-Lactam													
			AMP	AMP/SUL	PIP	PIP/TAZ	TIM/CLAV	AZT	FAZ	CRO	CAZ	FEP	ERT	IMI	MEM	DOR
E.coli (EC107) ST 131	CTX-M-15 (A), OXA-1 (D)	-	>16	>16/8	>64	>128/4	>64/2	>16	>16	>16	>16	>32	≤0.25	≤0.5	≤0.5	≤0.5
		+	>16	>16/8	>64	>128/4	64/2	≤1	8	<0.5	≤1	8	≤0.25	≤0.5	≤0.5	≤0.5
E.coli (EC114) ST 131	TEM-1 (A), CTX-M-15 (A), OXA-1 (D)	-	>16	>16/8	>64	>128/4	>64/2	>16	>16	>32	>16	>32	≤0.25	≤0.5	≤0.5	≤0.5
		+	>16	>16/8	>64	>128/4	>64/2	≤1	8	<0.5	≤1	8	≤0.25	≤0.5	≤0.5	≤0.5
E.coli (EC86)	CTX-M-15 (A), CMY-4 (C), OXA-181 (D)	-	>16	>16/8	>64	>128/4	>64/2	>16	>16	>16	>16	>32	>8	>8	4	>4
		+	>16	>16/8	>64	>128/4	>64/2	8	>16	8	8	≤4	4	4	1	2
E.coli (EC113) ST 131	CTX-M-27 (A)	-	>16	8/4	>64	≤8/4	16/2	>16	>16	>32	8	>32	≤0.25	≤0.5	≤0.5	≤0.5
		+	≤8	≤4/2	≤16	≤8/4	≤8/2	≤1	4	<0.5	≤1	≤4	≤0.25	≤0.5	≤0.5	≤0.5
K. pneumoniae (KP15)	TEM-1 (A), SHV-11 (A), KPC-2 (A)	-	>16	>16/8	>64	>128/4	>64/2	>16	>16	>32	>16	>32	>8	>8	>8	>4
		+	>16	16/8	>64	>128/4	>64/2	>16	>16	1	4	≤4	≤0.25	≤0.5	1	≤0.5
K. pneumoniae (KP41)	TEM-1 (A), SHV-1 (A), -5 (A), -11 (A), CTX-M-15 (A), OXA-232 (D)	-	>16	>16/8	>64	>128/4	>64/2	>16	>16	>32	>16	>32	>8	>8	>8	>4
		+	>16	>16/8	>64	>128/4	64/2	>16	>16	>32	>16	32	>8	>8	>8	>4
K. pneumoniae (KP58)	SHV-11 (A), VIM-4 (B)	-	>16	>16/8	>64	>128/4	>64/2	>16	>16	>32	>16	>32	>8	>8	>8	>4
		+	>16	>16/8	>64	>128/4	>64/2	2	>16	1	2	>32	≤0.25	2	≤0.5	≤0.5
P. stuartii (PS71)	TEM-1 (A), SHV-5 (A), VEB-1 (A), VIM-1 (B)	-	>16	>16/8	>64	>128/4	>64/2	>16	>16	>32	>16	>32	>8	>8	>8	>8
		+	>16	>16/8	>64	>128/4	>64/2	>16	4	16	>16	8	≤0.25	>8	1	2
P. aeruginosa (PA12) ST 111	VIM-2 (B)	-	>16	>16/8	>64	128/4	>64/2	>16	>16	>32	>16	>32	>8	>8	>8	>4
		+	>16	>16/8	64	128/4	>64/2	16	>16	>32	>16	>32	>8	>8	>8	>4
A. baumannii (AB14)	OXA-23 (D), OXA-51 (D)	-	>16	>16/8	>64	>128/4	>64/2	>16	>16	>32	>16	>32	>8	>8	4	>4
		+	>16	>16/8	>64	>128/4	>64/2	>16	>16	>32	>16	32	>8	>8	4	>4

Table 3. MIC values of selected penicillins, cephalosporins, monobactams, and carbapenems against different bacterial strains with or without cyclic boronate, 2, supplementation. MIC values in black indicate resistance and those in red suceptiobility according to current CLSI/EUCAST breakpoints. Blue values indicate where the MIC is reduced with 10 mg/L 2, but the MIC lies either outside of the susceptible range or there is no agreed breakpoint for the drug/organism combination. AMP: ampicillin; AMP/SUL: ampicillin/sulbactam; PIP: piperacillin; PIP/TAZ: piperacillin/tazobactam; TIM/CLAV: ticarcillin/clavulanate; AZT: aztreonam; FAZ: cefazolin; CRO: ceftriaxone; CAZ: ceftazidime; FEP: cefepime; ERT: ertapenem; IMI:imipenem; MEM: meropenem; DOR: doripenem.

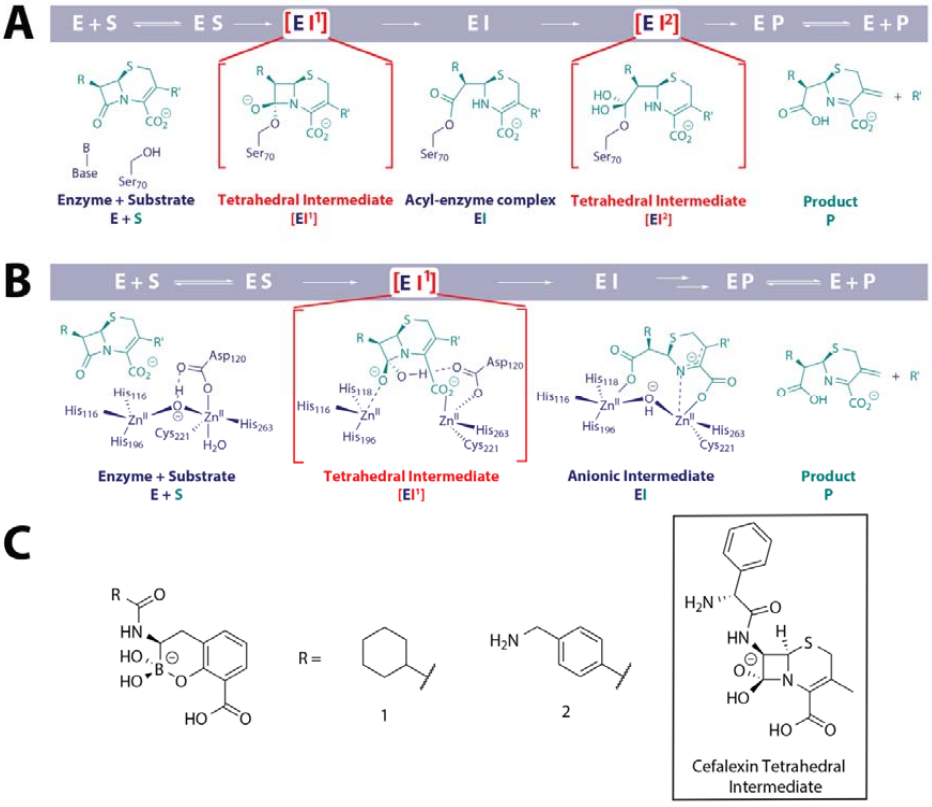

Figure 1. Outline mechanism of cephalosporin hydrolysis by (A) serine-β-lactamases and (B) metallo-β-lactamases. The small-molecule elements of the first tetrahedral intermediate EI^1 is common to both mechanisms. (C) Chemical structures of the two cyclic boronates used in this study. The structure of the proposed common tetrahedral intermediate in the serine and metallo-β-lactamase-catalysed hydrolysis of β-lactam antibiotics is shown for a cephalosporin substrate. We propose that the cyclic boronates mimic this intermediate.

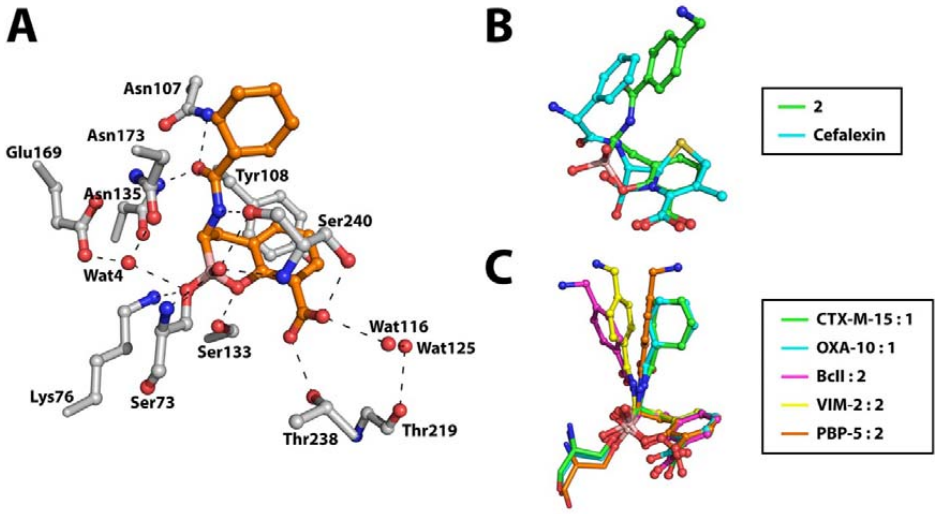

Figure 2. The conformation of the bicyclic ring core of the cyclic boronates in complex with β-lactamases and PBPs is conserved and mimics the tetrahedral anionic intermediate in cephalosporin hydrolysis. (A) Active site view from a crystal structure of the CTX-M-15:1 complex. Potential hydrogen bonding interactions are represented by dashed lines. (B) Overlay of energy minimised small-molecule structures of the cyclic boronate 2 and a modelled species defined by addition of a hydroxide ion onto the β-lactam carbonyl of cefalexin. Energy minimisation was carried out using the MM2 energy minimisation function in ChemBio3D Ultra. (C) Overlay of our reported (21) cyclic boronate structures in PDB entries 5FQ9 (cyan, OXA-10:1), 5FQB (magenta, BcII:2), 5FQC (yellow, VIM-2:2), 5J8X (orange, PBP-5:2) and our CTX-M-15:1 structure (green). Note that there is variation in the conformations of the side chain, but that of the fused bicyclic ring system is highly conserved in all crystal structures and is likely important for optimal binding of the cyclic boronate inhibitors.

References

1. **Versporten A, Bolokhovets G, Ghazaryan L, Abilova V, Pyshnik G, Spasojevic T, Korinteli I, Raka L, Kambaralieva B, Cizmovic L, Carp A, Radonjic V, Maqsudova N, Celik HD, Payerl-Pal M, Pedersen HB, Sautenkova N, Goossens H.** 2014. Antibiotic Use in Eastern Europe: A Cross-National Database Study in Coordination with the WHO Regional Office for Europe. Lancet Infect Dis **14:**381-387.
2. **Drawz SM, Bonomo RA.** 2010. Three Decades of β-Lactamase Inhibitors. Clin Microbiol Rev **23:**160-201.
3. **Bush K, Jacoby GA.** 2010. Updated Functional Classification of β-Lactamases. Antimicrob Agents Chemother **54:**969-976.
4. **Blair JMA, Webber MA, Baylay AJ, Ogbolu DO, Piddock LJV.** 2015. Molecular Mechanisms of Antibiotic Resistance. Nat Rev Microbiol **13:**42-51.
5. **Majiduddin FK, Materon IC, Palzkill TG.** 2002. Molecular Analysis of Beta-Lactamase Structure and Function. Int J Med Microbiol **292:**127-137.
6. **Massova I, Mobashery S.** 1998. Kinship and Diversification of Bacterial Penicillin-Binding Proteins and β-Lactamases. Antimicrob Agents Chemother **42:**1-17.
7. **Joris B, Ghuysen JM, Dive G, Renard A, Dideberg O, Charlier P, Frere JM, Kelly JA, Boyington JC, Moews PC, et al.** 1988. The active-site-serine penicillin-recognizing enzymes as members of the Streptomyces R61 DD-peptidase family. Biochem J **250:**313-324.
8. **Joris B, Ledent P, Dideberg O, Fonzé E, Lamotte-Brasseur J, Kelly JA, Ghuysen JM, Frère JM.** 1991. Comparison of the sequences of class A beta-lactamases and of the secondary structure elements of penicillin-recognizing proteins. Antimicrob Agents Chemother **35:**2294-2301.

9. **Paterson DL, Bonomo RA.** 2005. Extended-Spectrum β-Lactamases: a Clinical Update. Clin Microbiol Rev **18:**657-686.

10. **Pitout JDD, Laupland KB.** 2008. Extended-spectrum β-lactamase-producing Enterobacteriaceae: an emerging public-health concern. The Lancet Infectious Diseases **8:**159-166.

11. **Cantón R, Coque TM.** 2006. The CTX-M β-lactamase pandemic. Curr Opin Microbiol **9:**466-475.

12. **Evans BA, Amyes SGB.** 2014. OXA β-Lactamases. Clin Microbiol Rev **27:**241-263.

13. **Reading C, Cole M.** 1977. Clavulanic Acid: a Beta-Lactamase-Inhibiting Beta-Lactam from Streptomyces clavuligerus. Antimicrob Agents Chemother **11:**852-857.

14. **Yang Y, Rasmussen BA, Shlaes DM.** 1999. Class A β-lactamases—enzyme-inhibitor interactions and resistance. Pharmacol Ther **83:**141-151.

15. **Zhanel GG, Lawson CD, Adam H, Schweizer F, Zelenitsky S, Lagace-Wiens PR, Denisuik A, Rubinstein E, Gin AS, Hoban DJ, Lynch JP, 3rd, Karlowsky JA.** 2013. Ceftazidime-avibactam: a novel cephalosporin/beta-lactamase inhibitor combination. Drugs **73:**159-177.

16. **Ehmann DE, Jahić H, Ross PL, Gu R-F, Hu J, Durand-Réville TF, Lahiri S, Thresher J, Livchak S, Gao N, Palmer T, Walkup GK, Fisher SL.** 2013. Kinetics of Avibactam Inhibition against Class A, C, and D β-Lactamases. J Biol Chem **288:**27960-27971.

17. **Palzkill T.** 2013. Metallo-β-Lactamase Structure and Function. Ann N Y Acad Sci **1277:**91-104.

18. **Queenan AM, Bush K.** 2007. Carbapenemases: The Versatile β-Lactamases. Clin Microbiol Rev **20:**440-458.

19. **Abboud MI, Damblon C, Brem J, Smargiasso N, Mercuri P, Gilbert B, Rydzik AM, Claridge TDW, Schofield CJ, Frère J-M.** 2016. Interaction of Avibactam with Class B Metallo-β-lactamases. Antimicrob Agents Chemother doi:10.1128/aac.00897-16.

20. **Bush K.** 2015. A resurgence of β-lactamase inhibitor combinations effective against multidrug-resistant Gram-negative pathogens. Int J Antimicrob Agents **46:**483-493.

21. **Brem J, Cain R, Cahill S, McDonough MA, Clifton IJ, Jimenez-Castellanos J-C, Avison MB, Spencer J, Fishwick CWG, Schofield CJ.** 2016. Structural basis of metallo-β-lactamase, serine-β-lactamase and penicillin-binding protein inhibition by cyclic boronates. Nat Commun **7**.

22. **Berrow NS, Alderton D, Sainsbury S, Nettleship J, Assenberg R, Rahman N, Stuart DI, Owens RJ.** 2007. A versatile ligation-independent cloning method suitable for high-throughput expression screening applications. Nucleic Acids Res **35:**e45-e45.

23. **Woodford N, Carattoli A, Karisik E, Underwood A, Ellington MJ, Livermore DM.** 2009. Complete Nucleotide Sequences of Plasmids pEK204, pEK499, and pEK516, Encoding CTX-M Enzymes in Three Major Escherichia coli Lineages from the United Kingdom, All Belonging to the International O25:H4-ST131 Clone. Antimicrob Agents Chemother **53:**4472-4482.

24. **Holloway BW.** 1955. Genetic recombination in Pseudomonas aeruginosa. J Gen Microbiol **13:**572-581.

25. **Berrow NS, Alderton D, Owens RJ.** 2009. The precise engineering of expression vectors using high-throughput In-Fusion PCR cloning. Methods Mol Biol **498:**75-90.

26. **Inglis SR, Strieker M, Rydzik AM, Dessen A, Schofield CJ.** 2012. A boronic-acid-based probe for fluorescence polarization assays with penicillin binding proteins and β-lactamases. Anal Biochem **420:**41-47.

27. **Makena A, van Berkel SS, Lejeune C, Owens RJ, Verma A, Salimraj R, Spencer J, Brem J, Schofield CJ.** 2013. Chromophore-Linked Substrate (CLS405): Probing Metallo-β-Lactamase Activity and Inhibition. ChemMedChem **8:**1923-1929.

28. **Baurin S, Vercheval L, Bouillenne F, Falzone C, Brans A, Jacquamet L, Ferrer J-L, Sauvage E, Dehareng D, Frère J-M, Charlier P, Galleni M, Kerff F.** 2009. Critical Role of Tryptophan 154 for the Activity and Stability of Class D β-Lactamases. Biochemistry **48:**11252-11263.

584 29. **Golemi D, Maveyraud L, Vakulenko S, Samama JP, Mobashery S.** 2001. Critical involvement
585 of a carbamylated lysine in catalytic function of class D beta-lactamases. Proc Natl Acad Sci U
586 S A **98:**14280-14285.
587 30. **van Berkel SS, Brem J, Rydzik AM, Salimraj R, Cain R, Verma A, Owens RJ, Fishwick CWG,**
588 **Spencer J, Schofield CJ.** 2013. Assay Platform for Clinically Relevant Metallo-β-Lactamases. J
589 Med Chem **56:**6945-6953.
590 31. **Hornsey M, Phee L, Stubbings W, Wareham DW.** 2013. In vitro activity of the novel
591 monosulfactam BAL30072 alone and in combination with meropenem versus a diverse
592 collection of important Gram-negative pathogens. Int J Antimicrob Agents **42:**343-346.
593 32. **CLSI.** 2012. Methods for Dilution Antimicrobial Susceptibility Tests for Bacteria that Grow
594 Aerobically, Approved Standard, 9th ed. CLSI document M07-A9.
595 33. **Minor W, Cymborowski M, Otwinowski Z, Chruszcz M.** 2006. HKL-3000: the integration of
596 data reduction and structure solution - from diffraction images to an initial model in
597 minutes. Acta Crystallographica Section D **62:**859-866.
598 34. **Bunkoczi G, Echols N, McCoy AJ, Oeffner RD, Adams PD, Read RJ.** 2013. Phaser.MRage:
599 automated molecular replacement. Acta Crystallographica Section D **69:**2276-2286.
600 35. **Lahiri SD, Mangani S, Durand-Reville T, Benvenuti M, De Luca F, Sanyal G, Docquier J-D.**
601 2013. Structural Insight into Potent Broad-Spectrum Inhibition with Reversible Recyclization
602 Mechanism: Avibactam in Complex with CTX-M-15 and Pseudomonas aeruginosa AmpC β-
603 Lactamases. Antimicrob Agents Chemother **57:**2496-2505.
604 36. **Adams PD, Grosse-Kunstleve RW, Hung L-W, Ioerger TR, McCoy AJ, Moriarty NW, Read RJ,**
605 **Sacchettini JC, Sauter NK, Terwilliger TC.** 2002. PHENIX: Building New Software for
606 Automated Crystallographic Structure Determination. Acta Crystallogr Sect D Biol Crystallogr
607 **58:**1948-1954.
608 37. **Emsley P, Lohkamp B, Scott WG, Cowtan K.** 2010. Features and Development of Coot. Acta
609 Crystallogr Sect D Biol Crystallogr **66:**486-501.

610 38. **ChemBioDraw3DUltra.** PerkinElmer, Waltham, Massachusetts, USA.
611 www.cambridgesoft.com.

612 39. **O'Callaghan CH, Morris A, Kirby SM, Shingler AH.** 1972. Novel Method for Detection of β-
613 Lactamases by Using a Chromogenic Cephalosporin Substrate. Antimicrob Agents
614 Chemother **1:**283-288.

615 40. **Ehmann DE, Jahić H, Ross PL, Gu R-F, Hu J, Kern G, Walkup GK, Fisher SL.** 2012. Avibactam is
616 a covalent, reversible, non–β-lactam β-lactamase inhibitor. Proceedings of the National
617 Academy of Sciences **109:**11663-11668.

618 41. **Kalp M, Totir MA, Buynak JD, Carey PR.** 2009. Different intermediate populations formed by
619 tazobactam, sulbactam, and clavulanate reacting with SHV-1 β-lactamases: Raman
620 crystallographic evidence. J Am Chem Soc **131:**2338-2347.

621 42. **Imtiaz U, Billings EM, Knox JR, Mobashery S.** 1994. A Structure-Based Analysis of the
622 Inhibition of Class A β-Lactamases by Sulbactam. Biochemistry **33:**5728-5738.

623 43. **Ruzin A, Petersen PJ, Jones CH.** 2010. Resistance development profiling of piperacillin in
624 combination with the novel β-lactamase inhibitor BLI-489. J Antimicrob Chemother **65:**252-
625 257.

626 44. **Petersen PJ, Jones CH, Venkatesan AM, Bradford PA.** 2009. Efficacy of Piperacillin
627 Combined with the Penem β-Lactamase Inhibitor BLI-489 in Murine Models of Systemic
628 Infection. Antimicrob Agents Chemother **53:**1698-1700.

629 45. **Brem J, van Berkel SS, Zollman D, Lee SY, Gileadi O, McHugh PJ, Walsh TR, McDonough**
630 **MA, Schofield CJ.** 2016. Structural Basis of Metallo-β-Lactamase Inhibition by Captopril
631 Stereoisomers. Antimicrob Agents Chemother **60:**142-150.

632 46. **Yusof Y, Tan DTC, Arjomandi OK, Schenk G, McGeary RP.** 2016. Captopril analogues as
633 metallo-β-lactamase inhibitors. Bioorg Med Chem Lett **26:**1589-1593.

634 47. **Karsisiotis AI, Damblon CF, Roberts GCK.** 2013. Solution Structures of the *Bacillus cereus*
635 Metallo-β-Lactamase BcII and its Complex with the Broad Spectrum Inhibitor *R*-Thiomandelic
636 Acid. Biochem J **456:**397-407.
637 48. **Mollard C, Moali C, Papamicael C, Damblon C, Vessilier S, Amicosante G, Schofield CJ,**
638 **Galleni M, Frère J-M, Roberts GCK.** 2001. Thiomandelic Acid, a Broad Spectrum Inhibitor of
639 Zinc β-Lactamases: Kinetic and Spectroscopic Studies. J Biol Chem **276:**45015-45023.
640 49. **Maveyraud L, Golemi D, Kotra LP, Tranier S, Vakulenko S, Mobashery S, Samama JP.** 2000.
641 Insights into class D beta-lactamases are revealed by the crystal structure of the OXA10
642 enzyme from Pseudomonas aeruginosa. Structure **8:**1289-1298.
643 50. **King DT, King AM, Lal SM, Wright GD, Strynadka NCJ.** 2015. Molecular Mechanism of
644 Avibactam-Mediated β-Lactamase Inhibition. ACS Infectious Diseases **1:**175-184.
645 51. **Burns CJ, Goswami R, Jackson RW, Lessen T, Li W, Pevear D, Tirunahari PK, Xu H.** 2010.
646 Beta-lactamase inhibitors. WO 2010/130708 A1.
647 52. **Maveyraud L, Golemi-Kotra D, Ishiwata A, Meroueh O, Mobashery S, Samama J-P.** 2002.
648 High-Resolution X-ray Structure of an Acyl-Enzyme Species for the Class D OXA-10 β-
649 Lactamase. J Am Chem Soc **124:**2461-2465.
650 53. **Nukaga M, Abe T, Venkatesan AM, Mansour TS, Bonomo RA, Knox JR.** 2003. Inhibition of
651 Class A and Class C β-Lactamases by Penems: Crystallographic Structures of a Novel 1,4-
652 Thiazepine Intermediate. Biochemistry **42:**13152-13159.
653 54. **Bethel CR, Taracila M, Shyr T, Thomson JM, Distler AM, Hujer KM, Hujer AM, Endimiani A,**
654 **Papp-Wallace K, Bonnet R, Bonomo RA.** 2011. Exploring the Inhibition of CTX-M-9 by β-
655 Lactamase Inhibitors and Carbapenems. Antimicrob Agents Chemother **55:**3465-3475.
656 55. **Wang DY, Abboud MI, Markoulides MS, Brem J, Schofield CJ.** 2016. The road to avibactam:
657 the first clinically useful non-β-lactam working somewhat like a β-lactam. Future Medicinal
658 Chemistry **8:**1063-1084.

659 56. **Vshyvenko S, Clapson ML, Suzuki I, Hall DG.** 2016. Characterization of the Dynamic
660 Equilibrium between Closed and Open Forms of the Benzoxaborole Pharmacophore. ACS
661 Medicinal Chemistry Letters doi:10.1021/acsmedchemlett.6b00300.
662 57. **Gentile I, Maraolo AE, Borgia G.** 2016. What is the role of the new β-lactam/β-lactamase
663 inhibitors ceftolozane/tazobactam and ceftazidime/avibactam? Expert Review of Anti-
664 infective Therapy **14:**875-878.
665 58. **Hecker SJ, Reddy KR, Totrov M, Hirst GC, Lomovskaya O, Griffith DC, King P, Tsivkovski R,**
666 **Sun D, Sabet M, Tarazi Z, Clifton MC, Atkins K, Raymond A, Potts KT, Abendroth J, Boyer**
667 **SH, Loutit JS, Morgan EE, Durso S, Dudley MN.** 2015. Discovery of a Cyclic Boronic Acid β-
668 Lactamase Inhibitor (RPX7009) with Utility vs Class A Serine Carbapenemases. J Med Chem
669 **58:**3682-3692.
670 59. **Papp-Wallace KM, Bonomo RA.** 2016. New β-Lactamase Inhibitors in the Clinic. Infectious
671 disease clinics of North America **30:**441-464.
672 60. **Ness S, Martin R, Kindler AM, Paetzel M, Gold M, Jensen SE, Jones JB, Strynadka NCJ.** 2000.
673 Structure-Based Design Guides the Improved Efficacy of Deacylation Transition State
674 Analogue Inhibitors of TEM-1 β-Lactamase. Biochemistry **39:**5312-5321.
675 61. **Pernot L, Frenois F, Rybkine T, L'Hermite G, Petrella S, Delettre J, Jarlier V, Collatz E,**
676 **Sougakoff W.** 2001. Crystal structures of the class D beta-lactamase OXA-13 in the native
677 form and in complex with meropenem. J Mol Biol **310:**859-874.
678 62. **King DT, Worrall LJ, Gruninger R, Strynadka NC.** 2012. New Delhi metallo-beta-lactamase:
679 structural insights into beta-lactam recognition and inhibition. J Am Chem Soc **134:**11362-
680 11365.
681 63. **Feng H, Ding J, Zhu D, Liu X, Xu X, Zhang Y, Zang S, Wang DC, Liu W.** 2014. Structural and
682 mechanistic insights into NDM-1 catalyzed hydrolysis of cephalosporins. J Am Chem Soc
683 **136:**14694-14697.

64. **Elewski BE, Aly R, Baldwin SL, González Soto RF, Rich P, Weisfeld M, Wiltz H, Zane LT, Pollak R.** 2015. Efficacy and safety of tavaborole topical solution, 5%, a novel boron-based antifungal agent, for the treatment of toenail onychomycosis: Results from 2 randomized phase-III studies. Journal of the American Academy of Dermatology **73:**62-69.

65. **Nazarian R, Weinberg JM.** 2009. AN-2728, a PDE4 inhibitor for the potential topical treatment of psoriasis and atopic dermatitis. Curr Opin Investig Drugs **10:**1236-1242.

66. **Mendes RE, Alley MRK, Sader HS, Biedenbach DJ, Jones RN.** 2013. Potency and Spectrum of Activity of AN3365, a Novel Boron-Containing Protein Synthesis Inhibitor, Tested against Clinical Isolates of Enterobacteriaceae and Nonfermentative Gram-Negative Bacilli. Antimicrob Agents Chemother **57:**2849-2857.

Inhibitor	Pre-incubation Time (min)	TEM-1 IC_{50} (nM)	CTX-M-15 IC_{50} (nM)	AmpC IC_{50} (nM)	OXA-23 IC_{50} (nM)	OXA-48 IC_{50} (nM)
1	0	2.6 ± 0.1	92 ± 6	68 ± 3	220 ± 1	140 ± 1
	10	1.3 ± 0.1	13 ± 1	9.8 ± 0.3	250 ± 1	160 ± 1
	30	1.6 ± 0.1	3.7 ± 0.1	4.5 ± 0.1	260 ± 1	170 ± 1
	60	1.5 ± 0.1	1.7 ± 0.1	2.6 ± 0.1	270 ± 1	170 ± 1
	360	1.7 ± 0.1	4.0 ± 0.01	2.4 ± 0.1	730 ± 2	270 ± 1
2	0	8.1 ± 0.1	39 ± 2	270 ± 60	2000 ± 10	2000 ± 10
	10	3.4 ± 0.1	7.5 ± 0.3	120 ± 10	2600 ± 10	2600 ± 20
	30	2.6 ± 0.1	2.8 ± 0.1	150 ± 10	3300 ± 20	3400 ± 10
	60	2.6 ± 0.1	1.3 ± 0.1	100 ± 10	2600 ± 10	3000 ± 10
	360	2.1 ± 0.1	6.4 ± 0.1	96 ± 1	3300 ± 20	3300 ± 20
Sulbactam	0	860 ± 80	44 ± 1	$> 2 \times 10^5$	$> 2 \times 10^5$	$> 2 \times 10^5$
	10	600 ± 200	29 ± 1	42000 ± 2000	$> 2 \times 10^5$	$> 2 \times 10^5$
	30	600 ± 200	28 ± 7	8600 ± 600	$> 2 \times 10^5$	$> 2 \times 10^5$
	60	500 ± 200	32.0 ± 0.3	4400 ± 500	$> 2 \times 10^5$	$> 2 \times 10^5$
	360	700 ± 300	16.6 ± 0.1	1000 ± 400	$> 2 \times 10^5$	$> 2 \times 10^5$
Avibactam	0	19 ± 1	9.9 ± 0.2	1400 ± 400	770 ± 4	2500 ± 30
	10	3.4 ± 0.1	1.1 ± 0.1	190 ± 10	390 ± 1	810 ± 50
	30	2.2 ± 0.1	0.40 ± 0.06	200 ± 10	160 ± 2	300 ± 2
	60	2.0 ± 0.1	0.39 ± 0.01	200 ± 10	71 ± 1	150 ± 1
	360	4.3 ± 0.1	6.4 ± 0.1	150 ± 10	13 ± 1	20 ± 1
BLI-489	0	4.8 ± 0.2	32 ± 2	210 ± 20	5.6 ± 0.1	14 ± 1
	10	2.0 ± 0.1	6.9 ± 0.2	30 ± 1	5.6 ± 0.1	15 ± 1
	30	1.7 ± 0.2	2.2 ± 0.1	12.0 ± 0.4	6.2 ± 0.1	16 ± 1
	60	1.7 ± 0.1	0.94 ± 0.03	5.6 ± 0.1	8.6 ± 0.1	22 ± 1
	360	1.9 ± 0.1	8.0 ± 0.1	1.9 ± 0.1	18 ± 1	49 ± 1

Inhibitor	Pre-incubation Time (min)	BcII pH 7.5 IC_{50} (μM)	BcII pH 6.5 IC_{50} (μM)	VIM-1 pH 7.5 IC_{50} (μM)
1	0	2.8 ± 0.2	3.3 ± 0.1	1 ± 1
	10	3.0 ± 0.2	3.8 ± 0.2	1 ± 1.2
	30	2.8 ± 0.3	3.5 ± 0.1	1 ± 1.5
	60	3.4 ± 0.3	3.8 ± 0.2	1.4 ± 0.3
	360	3.1 ± 0.2	3.0 ± 0.2	1.2 ± 0.3
2	0	0.45 ± 0.02	0.27 ± 0.02	0.061 ± 0.001
	10	0.45 ± 0.02	0.20 ± 0.01	0.085 ± 0.002
	30	0.36 ± 0.02	0.20 ± 0.01	0.088 ± 0.001
	60	0.36 ± 0.01	0.20 ± 0.01	0.083 ± 0.002
	360	0.36 ± 0.03	0.23 ± 0.01	0.061 ± 0.001
L-Captopril	0	13.7 ± 0.3	17.4 ± 0.3	1.91 ± 0.06
	10	21 ± 1	20.4 ± 0.6	2.3 ± 0.2
	30	12.5 ± 0.5	16.8 ± 0.8	2.4 ± 0.2
	60	14.6 ± 0.4	13.7 ± 0.7	2.6 ± 0.1
	360	15 ± 1	16.3 ± 0.5	2.8 ± 0.2
(±)-TMA	0	0.30 ± 0.03	0.27 ± 0.06	0.38 ± 0.03
	10	0.39 ± 0.05	0.9 ± 0.1	0.45 ± 0.02
	30	0.33 ± 0.04	0.5 ± 0.1	0.8 ± 0.9
	60	0.5 ± 0.2	2 ± 1	1.4 ± 0.9
	360	2 ± 1	2 ± 1	2 ± 1

Bacterial Isolate	β-Lactmases Produced (Ambler Class)	± 2 Supplement (10 mg/L)	MIC (mg/L) for β-Lactam													
			AMP	AMP/SUL	PIP	PIP/TAZ	TIM/CLAV	AZT	FAZ	CRO	CAZ	FEP	ERT	IMI	MEM	DOR
E.coli (EC107) ST 131	CTX-M-15 (A), OXA-1 (D)	-	>16	>16/8	>64	>128/4	>64/2	>16	>16	>16	>16	>32	≤0.25	≤0.5	≤0.5	≤0.5
		+	>16	>16/8	>64	>128/4	64/2	≤1	8	<0.5	≤1	8	≤0.25	≤0.5	≤0.5	≤0.5
E.coli (EC114) ST 131	TEM-1 (A), CTX-M-15 (A), OXA-1 (D)	-	>16	>16/8	>64	>128/4	>64/2	>16	>16	>32	>16	>32	≤0.25	≤0.5	≤0.5	≤0.5
		+	>16	>16/8	>64	>128/4	>64/2	≤1	8	<0.5	≤1	8	≤0.25	≤0.5	≤0.5	≤0.5
E.coli (EC86)	CTX-M-15 (A), CMY-4 (C), OXA-181 (D)	-	>16	>16/8	>64	>128/4	>64/2	>16	>16	>16	>16	>32	>8	>8	4	>4
		+	>16	>16/8	>64	>128/4	>64/2	8	>16	8	8	≤4	4	4	1	2
E.coli (EC113) ST 131	CTX-M-27 (A)	-	>16	08-Apr	>64	≤8/4	16-Feb	>16	>16	>32	8	>32	≤0.25	≤0.5	≤0.5	≤0.5
		+	≤8	≤4/2	≤16	≤8/4	≤8/2	≤1	4	<0.5	≤1	≤4	≤0.25	≤0.5	≤0.5	≤0.5
K. pneumoniae (KP15)	TEM-1 (A), SHV-11 (A), KPC-2 (A)	-	>16	>16/8	>64	>128/4	>64/2	>16	>16	>32	>16	>32	>8	>8	>8	>4
		+	>16	16-Aug	>64	>128/4	>64/2	>16	>16	1	4	≤4	≤0.25	≤0.5	1	≤0.5
K. pneumoniae (KP41)	TEM-1 (A), SHV-1 (A), -5 (A), -11 (A), CTX-M-15 (A), OXA-232 (D)	-	>16	>16/8	>64	>128/4	>64/2	>16	>16	>32	>16	>32	>8	>8	>8	>4
		+	>16	>16/8	>64	>128/4	64/2	>16	>16	>32	>16	32	>8	>8	>8	>4
K. pneumoniae (KP58)	SHV-11 (A), VIM-4 (B)	-	>16	>16/8	>64	>128/4	>64/2	>16	>16	>32	>16	>32	>8	>8	>8	>4
		+	>16	>16/8	>64	>128/4	>64/2	2	>16	1	2	>32	≤0.25	2	≤0.5	≤0.5
P. stuartii (PS71)	TEM-1 (A), SHV-5 (A), VEB-1 (A), VIM-1 (B)	-	>16	>16/8	>64	>128/4	>64/2	>16	>16	>32	>16	>32	>8	>8	>8	>8
		+	>16	>16/8	>64	>128/4	>64/2	>16	4	16	>16	8	≤0.25	>8	1	2
P. aeruginosa (PA12) ST 111	VIM-2 (B)	-	>16	>16/8	>64	128/4	>64/2	>16	>16	>32	>16	>32	>8	>8	>8	>4
		+	>16	>16/8	64	128/4	>64/2	16	>16	>32	>16	>32	>8	>8	>8	>4
A. baumannii (AB14)	OXA-23 (D), OXA-51 (D)	-	>16	>16/8	>64	>128/4	>64/2	>16	>16	>32	>16	>32	>8	>8	4	>4
		+	>16	>16/8	>64	>128/4	>64/2	>16	>16	>32	>16	32	>8	>8	4	>4

Antimicrobial Agents and Chemotherapy